Supplemental Fig. 1

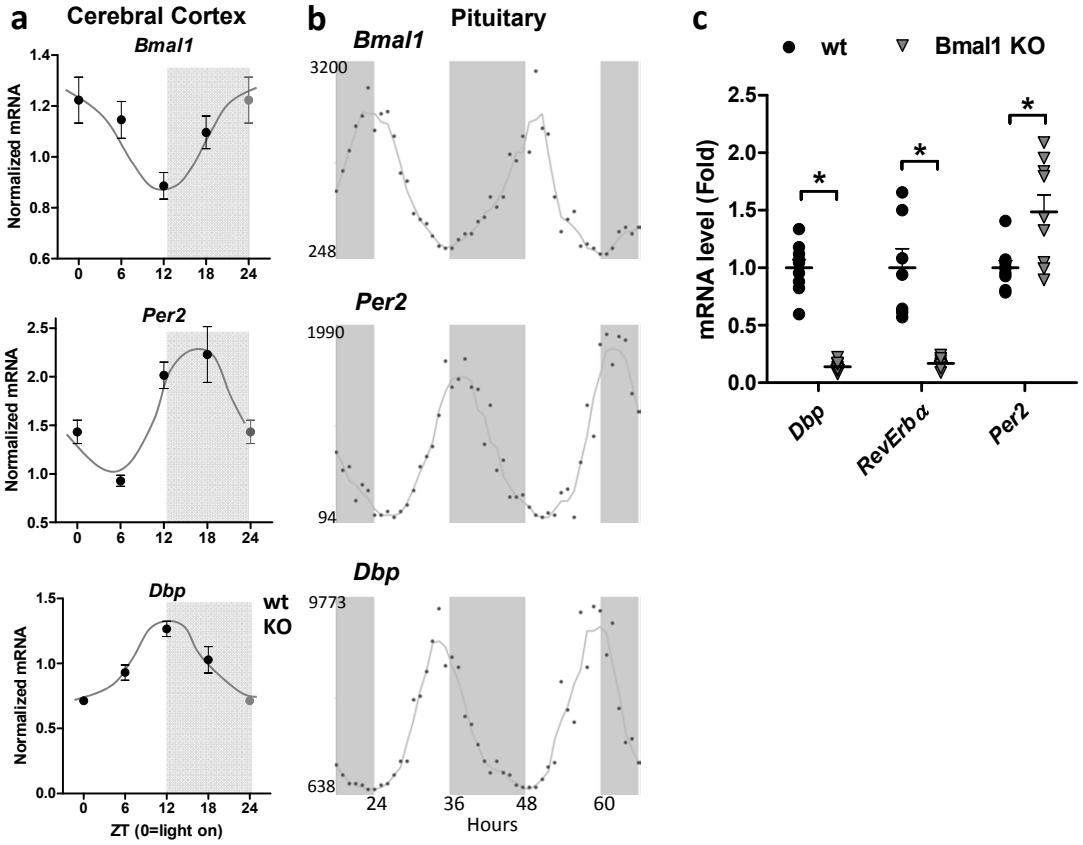

Supplemental Figure 1: Circadian oscillation of clock gene mRNA in mouse cerebral cortex. (a) Clock gene expression in cortex samples collected every 6 hours from 3mo wt mice kept in 12h:12h L:D conditions. N=3 mice per timepoint. Note that the ZT 24 timepoint (grey) is the ZT 0 timepoint shown again. (b) Circadian gene expression data from wt mice kept in constant darkness and sacrificed every 2 hours, from CircaDB. Relative expression levels (arbitrary units) is shown on y-axis. The JTK_CYCLE p-values for *Bmal1, Per2*, and *Dbp* in pituitary were all $<1x10^{-7}$. Note that the phase of *Bmal1* and *Bmal1* target (*Per2, Dbp*) expression is the same in cortex and other tissues. (c) Relative mRNA levels of Dbp, RevErba, and Per2 in B wt and Bmal1 KO cortex form mice sacrificed at ZT 3-8. N=7

Supplemental Fig. 2

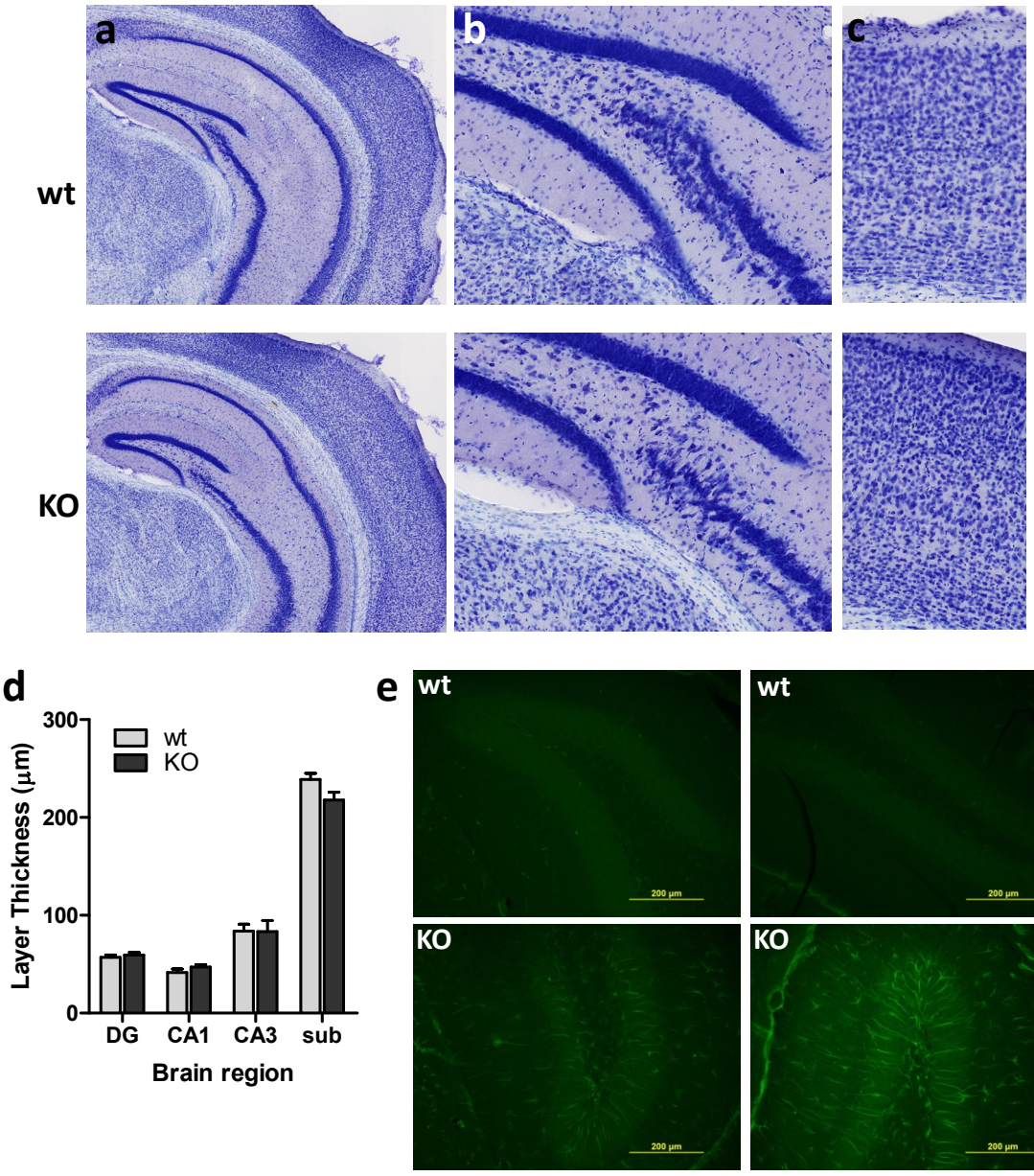

Supplemental Fig. 2: *Bmal1* KO brain is structurally normal at 6 mo and without major cell loss, but shows FluoroJade-positive cellular processes in hippocampus. Cresyl violet staining of hippocampus from 6 mo wt (upper) and *Bmal1* KO (lower) mice at 2.5x (a), and 10x (b) shows grossly normal structure and no obvious loss of neurons from dentate gyrus or CA3. Sections through retrospenial cortex (c) also show no neuronal loss at this age. (d) Measurement of thickness of nuclei layers in the dentate gyrus, CA1, CA3, and subiculum show no evidence of cell loss. Measurements were performed on 3-5 sections/mouse on brains from 3 mice/genotype. (e) FluoroJade C staining of hippocampal sections from 6mo wt and Bmal1 KO mice reveals numerous positive cellular processes in *Bmal1* KO mice.

Supplemental Fig. 3

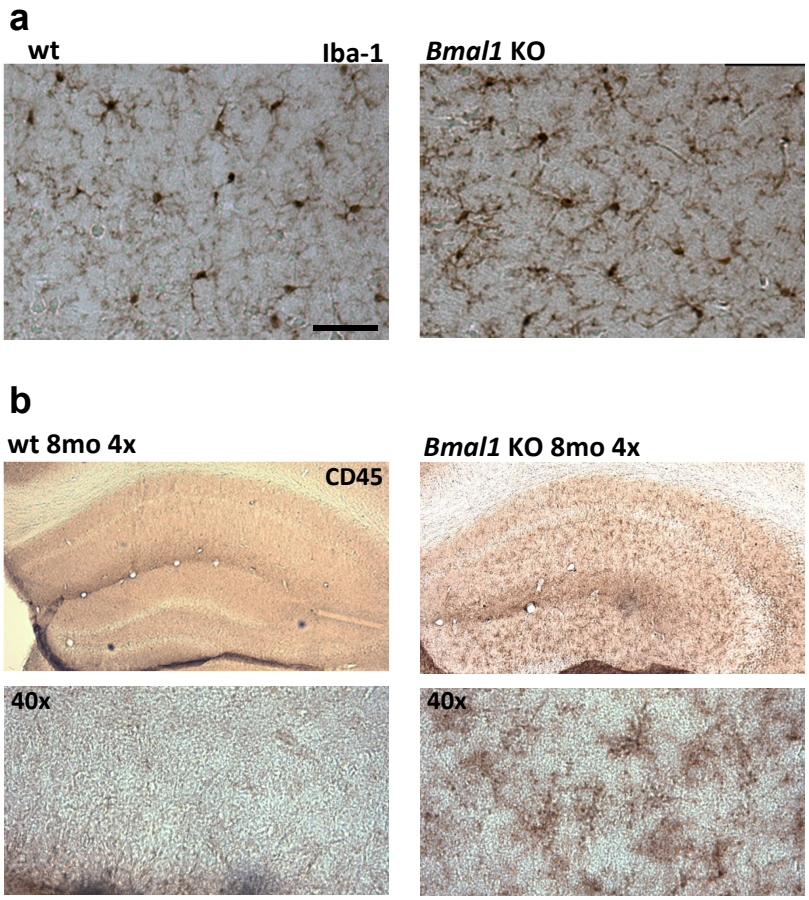

Supplemental Fig. 3: Mildly increased microglial activation in *Bmal1* KO brain at older ages. (a) Representative image of Iba1 staining of 6mo wt or *Bmal1* KO retroslpenial cortex shows a slight increase in microglial activation. Scale bar: 100um. (b) Increased activated microglia identified by CD45 staining in hippocampus of an 8mo Bmal1 KO mouse. Of note, no increases in CD45 immunoreactivity were observed in younger *Bmal1* KO mice.

Supplemental Fig. 4

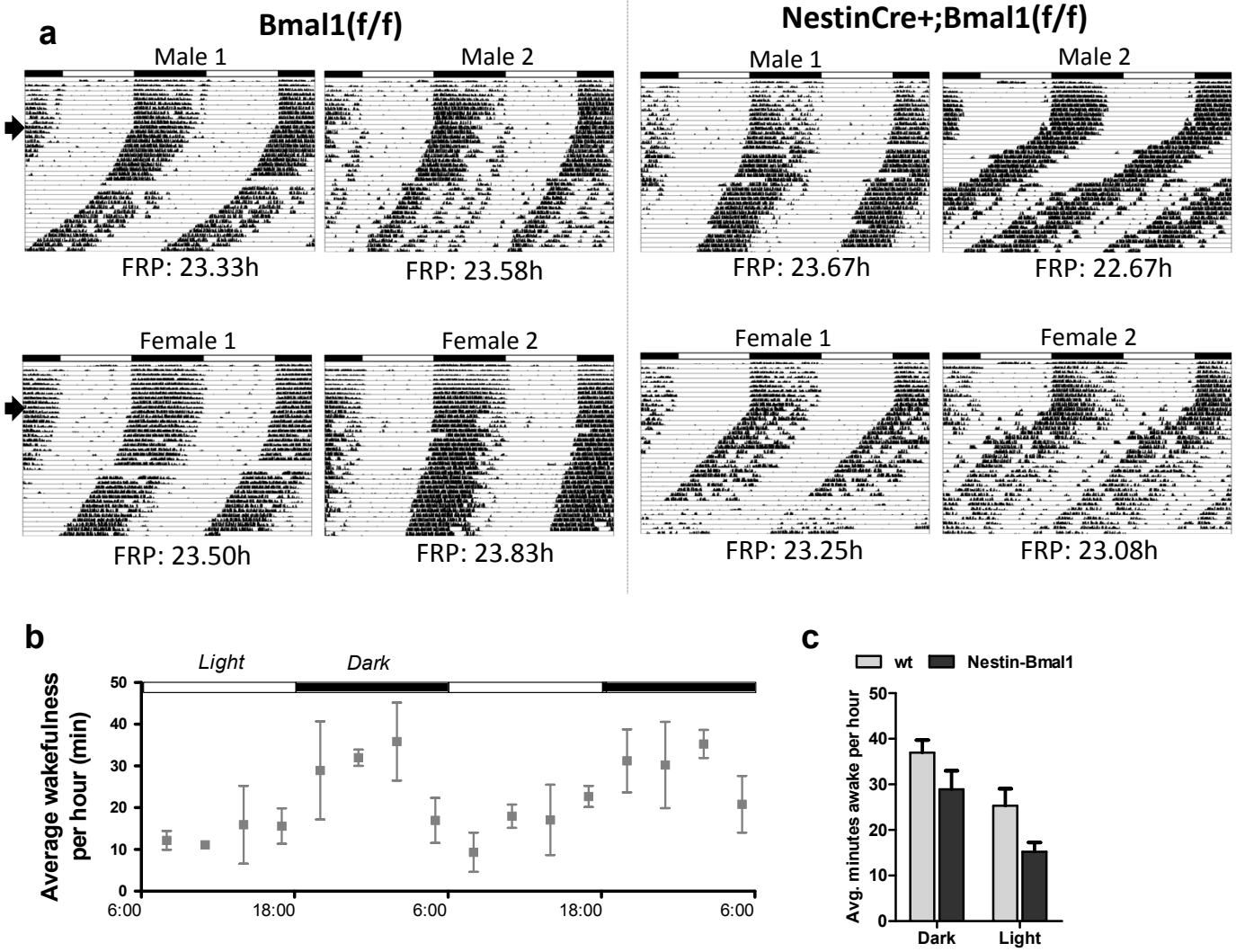

Supplemental Fig. 4: NestinCre+;Bmal1(f/f) have intact systemic circadian rhythms and sleep-wake oscillation.

(a) Actograms from all mice tested showing wheel running activity in two 3-4mo Bmal1$^{flox/flox}$ control and NestinCre+;Bmal1(f/f) mice. Each panel shows data from a representative mouse, recorded for 10 days in 12h:12h light:dark, then 30 days in constant darkness (start of constant darkness denoted by arrowhead). Free running period is listed for each actogram. (b,c). Sleep-wake analysis on NestinCre+;Bmal1(f/f) mice. (b) Average number of minutes of wakefulness per hour, as assessed by EEG analysis, for n=2 NestinCre+;Bmal1(f/f) mice shows diurnal oscillation when plotted in 3-hour intervals (b) and when averaged over 24 hours (c). For comparison, average minutes of wakefulness per hour for n=2 wt C57Bl6 mice analyzed in our laboratory is shown in (c). The difference between average minutes awake per hour between light and dark was 11.6 min for wt, 13.5 for NestinCre+;Bmal1(f/f) mice.

Supplemental Fig. 5

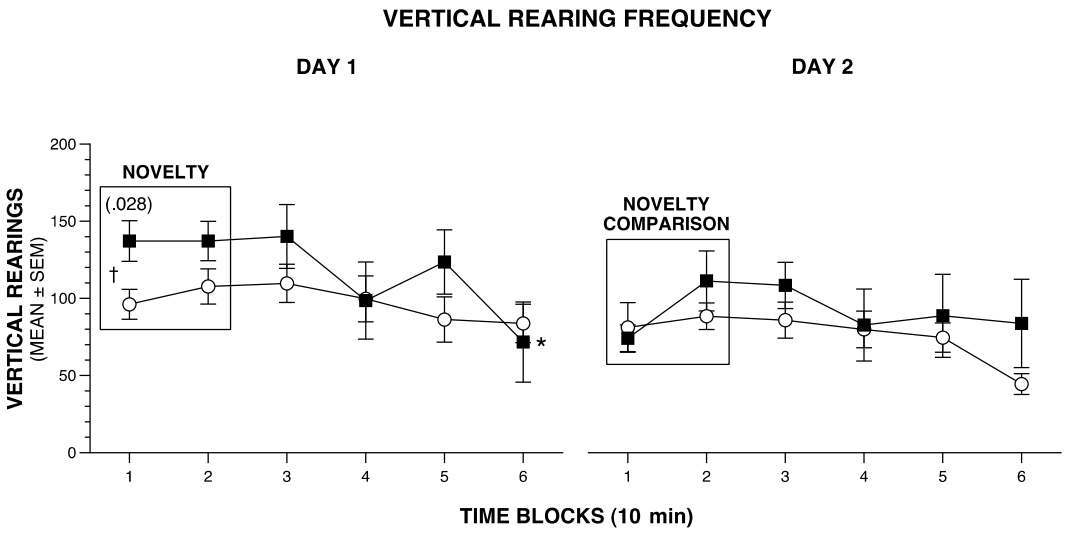

Supplemental Fig. 5: Increased novelty-induced vertical rearings in NestinCre+;Bmal1(f/f) mice. The number of vertical rearings were evaluated in the NestinCre+;Bmal1(f/f) (n=7) and Control (n=7) mice over a 1-h period on two consecutive days as in Fig. 4h. NestinCre+;Bmal1(f/f) mice showing increased numbers of rearings compared to the WT controls for block 1 (p=0.028 by rmANOVA). *p=0.12 for NestinCre+;Bmal1(f/f) when comparing rearing frequencies during block 1 versus block 6.

Supplemental Fig. 6

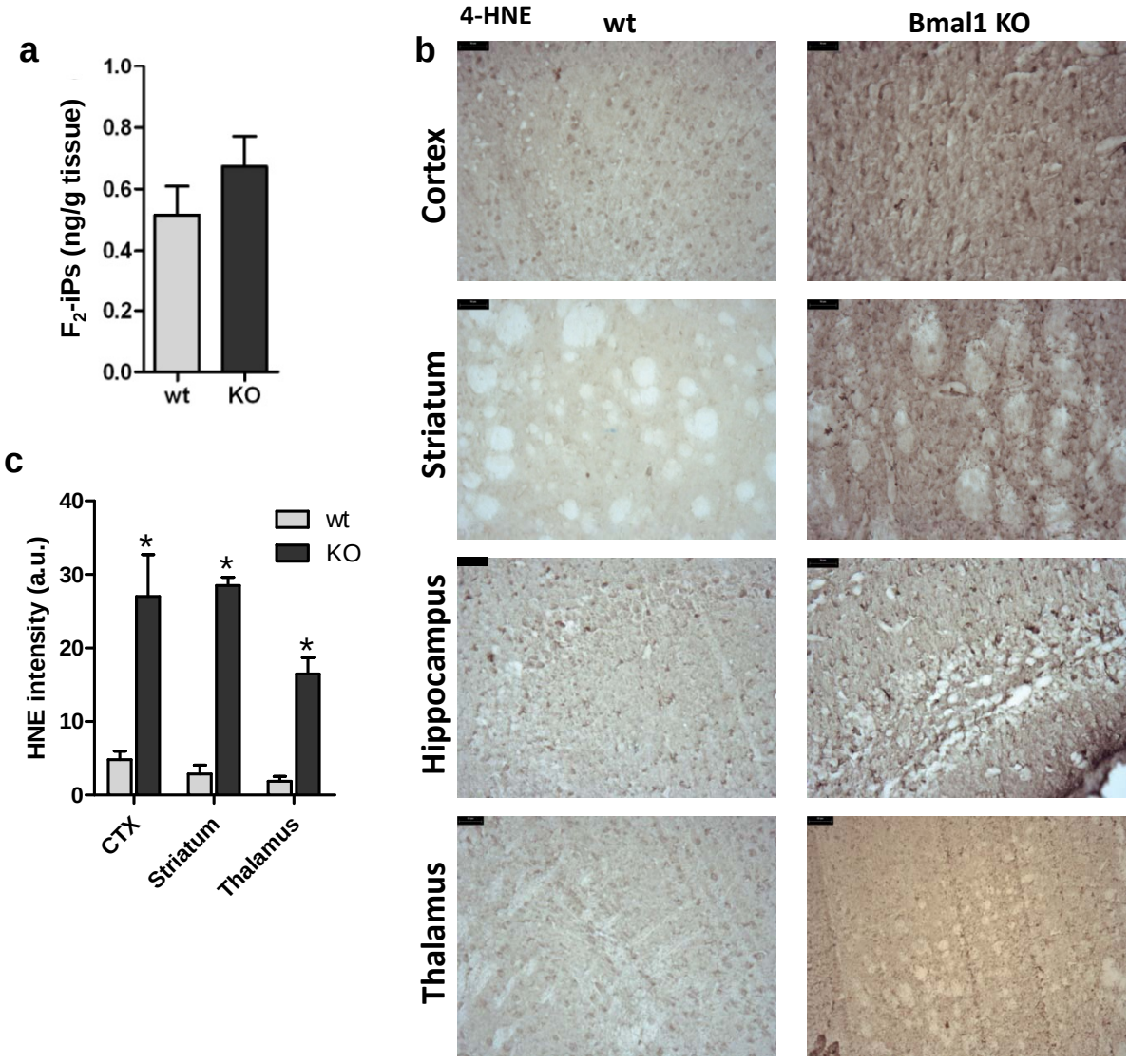

Supplemental Fig. 6: F2-Isoprostane and 4-hydroxynonenal in Bmal1 KO brain. (a) F2-isoprostane (F2-iP) levels in 6mo Bmal1 KO cortex show a non-significant trend toward increase. N=5 mice/genotype. (b) Immunostaining for 4-hydroxynonenal Michael Adducts in various brain regions from wt and Bmal1 KO brain. (c) Quantification of 4-HNE staining intensity. N=3-4 mice/genotype, *p<0.05 by 2-way ANOVA with Bonferroni correction, as compared to wt for that brain region. Scale bars, 50um.

Supplemental Fig. 7

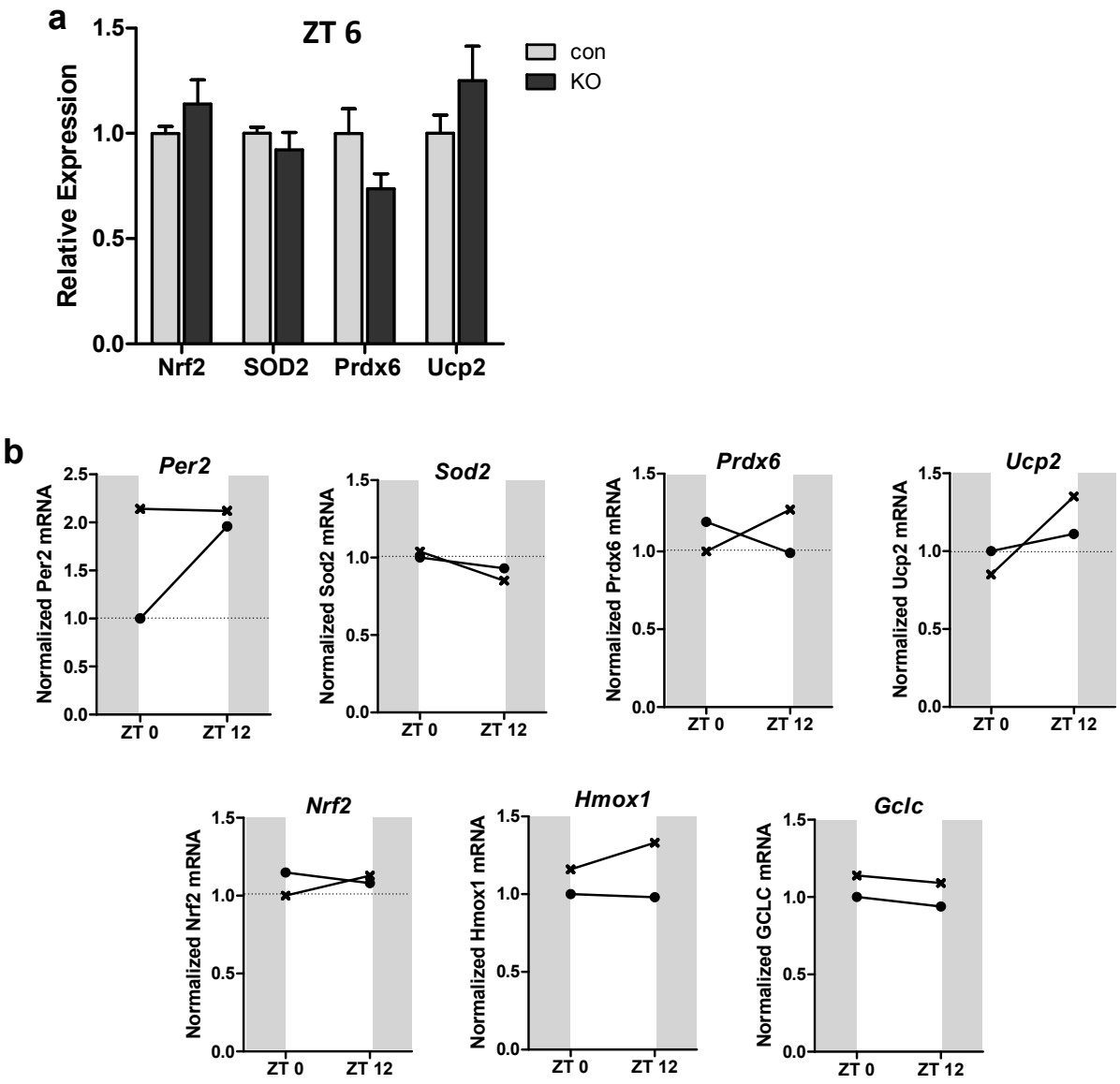

Supplemental Fig. 7: Analysis of candidate redox gene regulation in Bmal1 KO and NestinCre+;Bmal1(f/f) cortex. (a) No significant changes in mRNA level as assessed by qPCR of several candidate redox genes in 6mo Bmal1 KO cortex vs. wt at ZT 6. N=5 mice/genotype. (b) Analysis of mRNA levels of candidate redox genes in NestinCre+ (black circles) and NestinCre+;Bmal1(f/f) cortex (x) at ZT 0 and 12. No clear alteration in expression pattern of *Sod2*, *Prdx6*, *Ucp2*, or *Nrf2* was noted. The Nrf2 target genes *Hmox1* and *Gclc* were increased in NestinCre+;Bmal1(f/f) cortex at both timepoints, suggesting appropriate transcriptional response of these genes to oxidative stress. For (b), each point is the average value of 2 animals/genotype/timepoint. Of note, Per2 expression is higher at ZT 0 in Bmal1 KOs, perhaps due to loss of repression by RevErba.

Supplemental Fig. 8

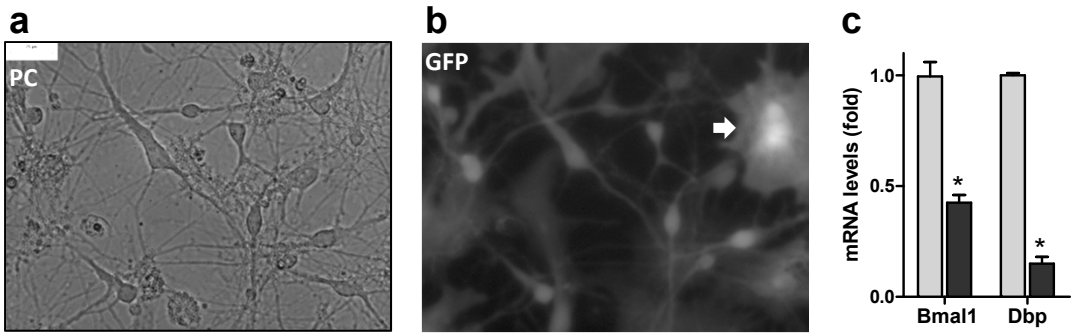

Supplemental Fig. 8: Representative lentiviral infection and GFP expression in primary neuronal cultures. DIV 5 primary mouse neuron-enriched cultures were treated for 24 hrs with lentivirus expressing shBMAL1 and GFP. (a) Live-cell phase contrast (PC) and (b) fluorescence (GFP) images show GFP expression in the vast majority of neurons, and in an astrocyte (arrow). No background fluorescence was observed in non-infected cells. Scale bar=25um. (c) *Bmal1* and *Dbp* mRNA levels in primary neurons 3 days after treatment with LV-scrambled (grey bars) or LV-shBmal1 (black bars) lentivirus. *p<0.05 by 2-way ANOVA with Bonferroni post-test.

Supplemental Fig. 9

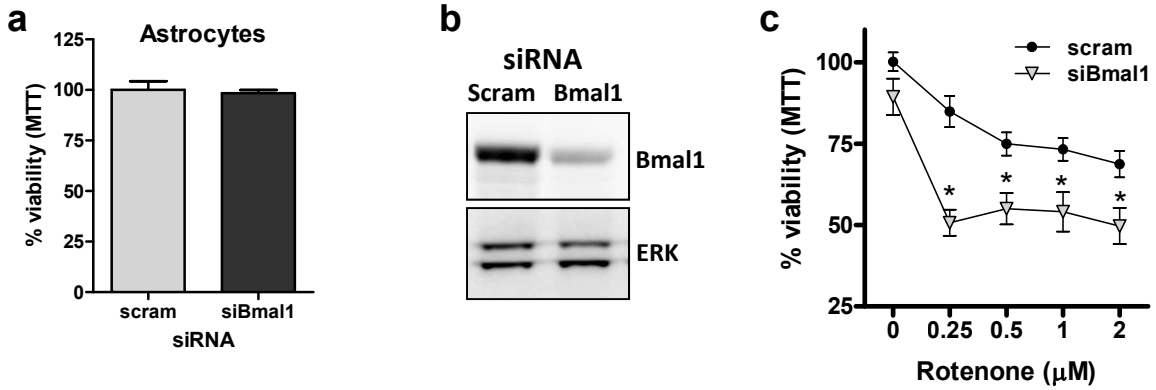

Supplemental Fig. 9: siRNA knockdown of *Bmal1* does not alter viability in primary astrocytes, but does sensitize Neuro2a cells to rotenone toxicity. (a) Primary mouse astrocytes were transfected with scrambled siRNA (scram) or *Bmal1* siRNA, and cell viability was assessed by MTT assay 3 days later. (b) Transfection of Neuro2a neuroblastoma cells with scrambled siRNA (scram) or *Bmal1* siRNA causes a marked decrease in BMAL1 protein, as assessed by western blot. Cells were harvested 2 days after transfection. (c) Neuro2a cells transfected as in (b) were treated with increasing concentrations of the mitochondrial complex I inhibitor rotenone, and viability was assessed by MTT assay 24 hours later. Each point is the mean+SEM of 3 independent experiments, *p<0.05 vs. scrambled siRNA at the same drug concentration by 2-way ANOVA.

Supplemental Fig. 10

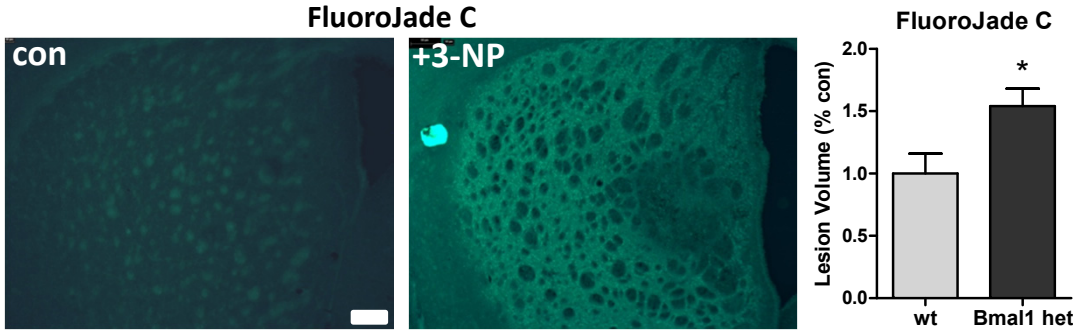

Supplemental Fig. 10: Striatal FluoroJade C staining in 3-nitropropionic acid treated mouse brain. Left panels: Representative image of a section from *Bmal1* +/- mouse brain showing typical FluoroJade C (FJ) staining of degenerating neurons and neuronal processes in the striatum 3 days after intrastriatal injection of vehicle (con) or 3-NP. No FJ staining was observed outside the striatum. Scale bar=100um. Right panel: Lesion volume quantified by FJ staining in 3-NP treated WT and *Bmal1* hemizygous mice from Figure 8. *p<0.05 by 2-tailed t-test.

Supplemental Table 1

		Bmal1 KO				Bmal1 KO
Gene	Oscillation	pituitary		**Gene**	Oscillation	pituitary
Uncoupling proteins	JTK p<0.05	p-value		Superoxide Dismutases	JTK p<0.05	p-value
Ucp1		ns		Sod1		
Ucp2	**yes**	**ns**		**Sod2**	**yes**	**0.08**
Ucp3		ns		Sod3		
				Ccs		
Peroxiredoxins						
Prdx1		ns		Catalase		
Prdx2		ns				
Prdx3		ns		Thioredoxins		
Prdx4		ns		**Txnip**	**yes**	**ns**
Prdx5	**yes**	ns		Txnrd1		**0.013**
Prdx6	**yes**	**0.052**		Txnrd2		ns
				Txnrd3	**yes**	**ns**
Aldehyde dehydrogenases				Txn1		ns
ALDH3b1	**yes**	**ns**		Txn2		**0.03**
ALDH1l2	**yes**	**ns**		Txn3		
ALDH1b1		ns				
ALDH1a2		0.009		Glutathione-related		
ALDH1a1		ns		**Gclc**	**yes**	ns
ALDH3a1		ns		**Gclm**	**yes**	ns
ALDH3a2		ns		Gpx1		ns
ALDH18a1		0.034		Gpx2		ns
ALDH9a1		ns		Gpx3		ns
ALDH2		**0.0011**		Gpx4		ns
ALDH6a1		0.02		Gpx5		ns
ALDH3b2		ns		Gpx6		ns
				Gpx7		ns
nrf2	**yes**	**0.02**		Gpx8		ns
NQO1		ns		Gss		ns
Hmox1		ns		Gsr		ns
Keap1		ns		GSTa1		ns
g6pdx		ns		GSTa2		ns
				GSTa3		ns
NAD(P)H Oxidases				**GSTa4**	**yes**	**0.06**
Nox1		ns		GSTa5		ns
Nox2		ns		GSTk1		ns
Nox3		ns		**GSTm1**		**0.01**
Nox4		ns		GSTm2		ns
Noxo1		ns		GSTm3		ns
Ndor1		ns		**GSTm4**	**yes**	ns
				GSTm5		ns
Sirtuins				GSTm6		ns
SirT1		ns		**GSTm7**		**0.003**
SirT2		ns		**GSTo1**	**yes**	**0.03**
SirT3		ns		**GSTp1**	**yes**	ns
SirT4		ns		GSTp2		ns
SirT5		ns		GSTt1		0.002
SirT6		ns		**GSTt2**	**yes**	ns
SirT7		ns		GSTt3		ns
				MGST1		0.03
				MGST2		ns
				MGST3		ns

Supplemental Methods:

Behavioral Testing: General locomotor activity and exploratory behaviors were evaluated in the NestinCre+;Bmal1 (f/f) (n=7) and Control (n=7) mice over a 1-h period on two consecutive days using transparent (47.6 x 25.4 x 20.6 cm high) polystyrene enclosures and computerized photobeam instrumentation, as previously described (1). Total ambulations (whole body movements), and vertical rearings were analyzed over the two test days. Repeated measures (rm) ANOVA models containing one between-subjects variable (Genotype) and two within-subjects (repeated measures) variables (Time Blocks and Test Days) were used to analyze the total ambulations and vertical rearing data. Sex was not included in the ANOVA model due to small sample sizes although the same sex distribution was maintained across the two groups. The Huynh-Feldt adjustment of alpha levels was utilized for all within-subjects effects containing more than two levels to protect against violations of sphericity/compound symmetry assumptions underlying rmANOVA models. Planned comparisons were conducted over the first two time blocks on both test days to evaluate novelty. Performance during block 1 compared to levels observed during block 6 was also conducted in each group and for each test day to assess habituation. Bonferroni correction was used when appropriate following multiple comparisons.

Transmission electron microscopy: Six month old mice (3 *Bmal1* KO and 3 wt) were anesthetized with pentobarbital and perfused transcardially with phosphate buffered saline for 1 minutes, then with a fixative composed of 2.5% glutaraldehyde and 2% paraformaldehyde in 0.1 M cacodylate buffer (pH 7.4). The brains were fixed overnight in the same buffer. Brains were cut into 1mm sections, then postfixed overnight in 1% osmium tetroxide. Tissue was dehydrated in graded solutions of ethanol from 40% to 100% (each for 10 min), cleared in propylene oxide, and flat-embedded in araldite. Ultrathin sections were cut with a Leica Ultracut UCT ultramicrotome. Sections were counterstained with saturated aqueous uranyl acetate, followed by lead citrate and analyzed with a JEOL 100CX transmission electron microscope.

Chromatin Immunoprecipitation (ChIP): For in vivo ChIP analysis, brain cortex tissues were collected from mice and the following experimental procedures to prepare chromatin were performed as previously described (2). The pre-cleared chromatin was immunoprecipitated for 5 hours at 4°C by agitating with 4 µg of anti-BMAL1 antibody (A302-616A, Bethyl Laboratories) and normal rabbit IgG as a negative control antibody (#2729, Cell Signalling Technology). The lysates without incubation of antibody were used for input control. Immune complexes were collected by incubation with protein-G coated magnetic beads (Life Technologies) and the final eluted DNA was extracted by phenol-chloroform-isoamyl alcohol (25:24:1) and ethanol precipitation. The primer sets used for ChIP PCR analysis of the targeted gene promoter regions spanning canonical (CACGTG) or non-canonical E-box elements (CCAATG, CATTGG. CACGTT) were as follows: for canonical E-box region located upstream of *Nrf2* promoter (-892/-729), p*Nrf2* E-Box forward primer, 5'-TCCACTTCGGTGATTCTGTT -3' and reverse E-box1 primer, 5'-AGGGAGATGGATGAGTCCAC -3' (amplified 168 bp); For canonical E-box region located upstream of *Aldh2* promoter (-2466/-2265), p*Aldh2* E-Box forward primer, 5'- TGTGTCCATCAGGAACTGTC-3' and reverse E-box1 primer, 5'- GCCGTGCTGTAAATCCTACT -3' (amplified 201 bp); For non canonical E-box cluster region located upstream of *Nqo1* promoter (-1922/-1474), p*Nqo1* E-Box forward primer, 5'- TCTCCAGTGTACCCACCTCT-3' and reverse E-box1 primer, 5'-AGGAGCTGGGGATATAGCTT-3' (amplified 449 bp).

Mass spectrometric analysis of F_2-isoprostanes and F_4-neuroprostanes: 50-100mg samples of mouse cerebral cortex tissue were mechanically homogenized in 2:1 chlorofolm:methanol solution containing BHT (0.005%) and extracted with NaCl and 1ng of d_4-8,12-iso-iPF$_{2\alpha}$-VI internal standard was added. Samples were dried under nitrogen, then resuspended in 200mL methanol+butylated hydroxytolulene, followed by saponification with the addition of 200mL of 15% KOH and incubation at 37 degrees C for 20 minutes. Sample pH was then adjusted to 3 with formic acid, and samples were then centrifuged at 13,000 x g for 5 minutes and all floating precipitate was discarded. Total sample volume was adjusted to 4ml, and samples were subjected to solid-phase extraction using StrataX cartridges (Phenomenex, Torrance, CA) which were conditioned with 4ml acetonitrile (ACN) and 3 ml water, loaded with sample, then washed with 5ml 5% ACN in water, followed by elution with 5% ACN in ethyl acetate. Samples were then dried under nitrogen, reconstituted in 200 µl of 20% acetonitrile in water, and filtered by centrifugation. Liquid chromatography/tandem mass spectrometric analysis was performed as previously described (61) on a TSQ Quantum triple quadrupole analyzer operating in selected reaction monitoring mode. The ion transitions of interest were as follows: endogenous F_4-neuroprostanes, *m/z* 377→113; endogenous F_2-isoprostanes (8,12-iso-iPF$_{2\alpha}$-VI), *m/z* 353→115; tetradeuterated isoprostane internal standard (d_4-8,12-iso-iPF$_{2\alpha}$-VI), *m/z* 357→115.

FluoroJade C staining: FluoroJade C was purchased from EMD Millipore (Billerica, MA). 50um brain sections were mounted on gelatin-coated slides and dried overnight. Slides were incubated in PBS for 5 minutes, then 1% NaOH in 80% ethanol for 5 minutes, then 70% ethanol for 2 minutes. After a wash in PBS, slides were incubated in 0.06% potassium permanganate solution for 15 minutes, washed in PBS, the 30 minutes in 0.001% FluoroJade C in 0.1% acetic acid. Slides were washed, dried thoroughly, immersed in xylene twice, then coverslipped with DPX mounting media.

Sleep wake cycle analysis: EEG and EMG recordings were obtained as previously described (3) in Nestin-Cre::Bmal1$^{f/f}$ mice (8mo) housed in 12h L:D conditions. Mice were habituated to the recording cages for 3 days, then recording was performed for 3 days. EEG/EMG records were scored semiautomatically using a sleep scoring software (SleepSign, Kissei Comtec Co., LTD., Japan) into 10-sec epochs as Awake, REM, and NREM on the basis of standard criteria of rodent sleep. This preliminary scoring was confirmed visually.

Supplemental References:

1. Wozniak, D.F., Hartman, R.E., Boyle, M.P., Vogt, S.K., Brooks, A.R., Tenkova, T., Young, C., Olney, J.W., and Muglia, L.J. Apoptotic neurodegeneration induced by ethanol in neonatal mice is associated with profound learning/memory deficits in juveniles followed by progressive functional recovery in adults. *Neurobiol Dis.* 2004; 17(3):403-414.
2. Schmidt, D., Wilson, M.D., Spyrou, C., Brown, G.D., Hadfield, J., and Odom, D.T. ChIP-seq: using high-throughput sequencing to discover protein-DNA interactions. *Methods.* 2009; 48(3):240-248.
3. Kang, J.E., Lim, M.M., Bateman, R.J., Lee, J.J., Smyth, L.P., Cirrito, J.R., Fujiki, N., Nishino, S., and Holtzman, D.M. Amyloid-beta dynamics are regulated by orexin and the sleep-wake cycle. *Science.* 2009; 326(5955):1005-1007.